LA-UR-12-23050
Approved for public release; distribution is unlimited.

Title: Radiation Induced Defects Behavior in the Presence of Interfaces

Author(s): Martinez Saez, Enrique
Caro, Jose A.
Uberuaga, Blas P.

Intended for: CAARI 2012 22nd International Conference on the Application of Accelerators in Research and Industry, 2012-08-06/2012-08-10 (Fort Worth, Texas, United States)

Radiation Induced Defects Behavior in the Presence of Interfaces

Enrique Martinez, Blas Uberuaga and Alfredo Caro

MST-8, CMIME, Los Alamos National Laboratory, Los Alamos, New Mexico 87545, USA

CMIME IE Thrust

Outline

- **Motivation**
- **Coherent Interfaces**
  - Effect of $\Delta\mu$ and ΔE on defect accumulation and recombination
- **Semi-coherent Interfaces**
  - Development of an off-lattice kinetic Monte Carlo code
    - Why we need this kind of code
    - What we can do with it (so far)
  - Applications. Vacancy diffusion in the presence of Twist Boundaries
  - Error Estimation
- **Conclusions**

Radiation damage at “structureless” interfaces

- “Structureless" in this context refers to interfaces where
  - the response is dominated by defect energetics and kinetics
  - with only a minor contribution from the interface atomic structure.
- Such interfaces are likely to be coherent or nearly-coherent with a small lattice mismatch.

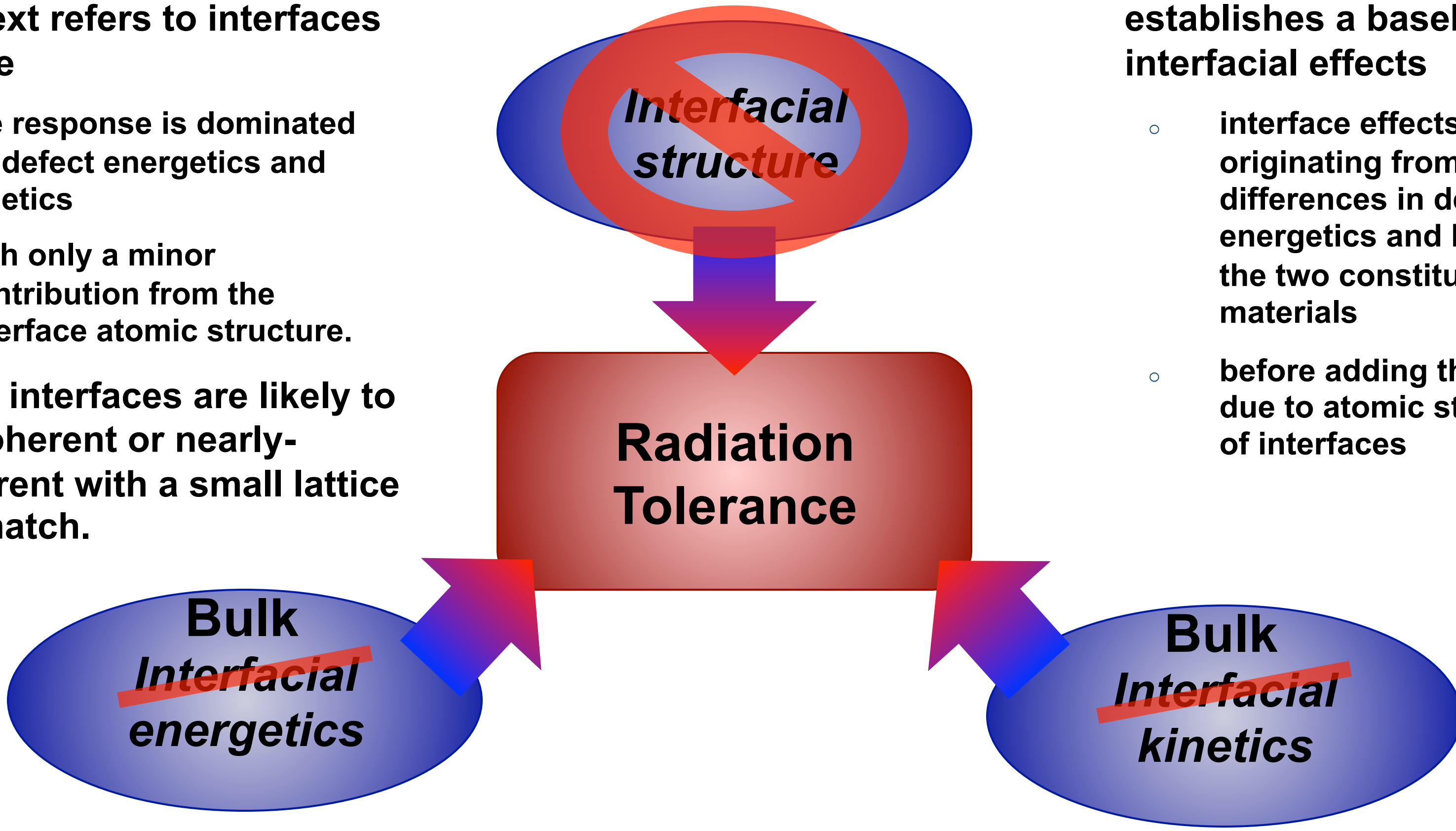

- Study of such interfaces establishes a baseline for interfacial effects
  - interface effects originating from differences in defect energetics and kinetics in the two constituent materials
  - before adding the effects due to atomic structures of interfaces

The atomic structure of the $TiO_2/SrTiO_3$ interface

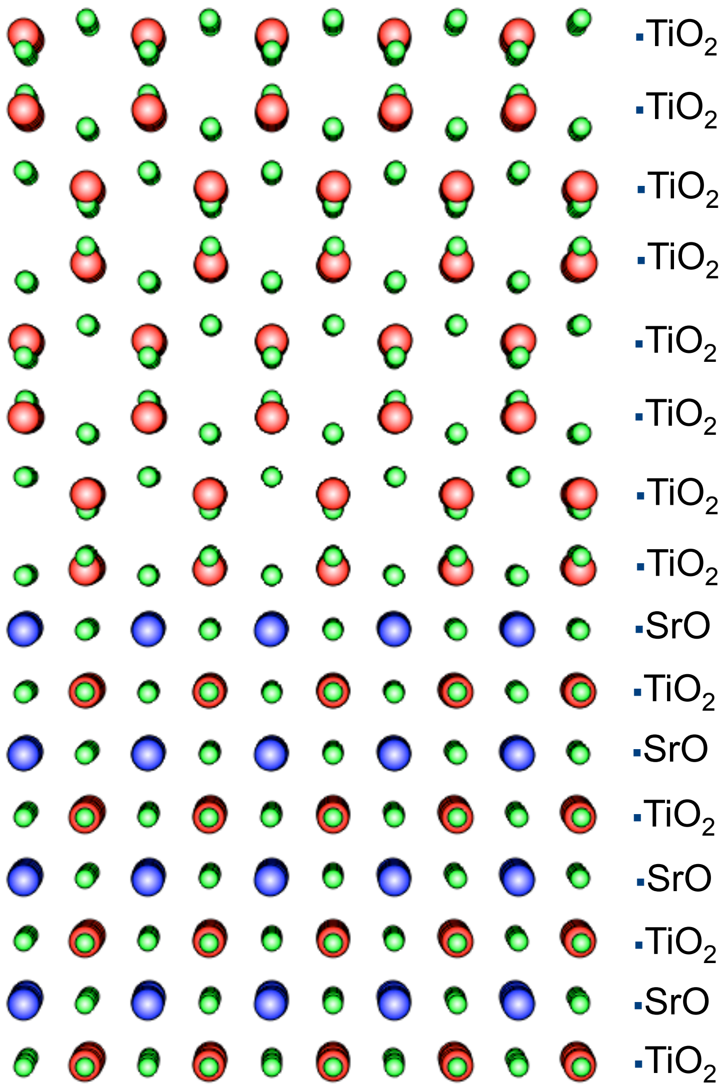

- **(001) direction of $SrTiO_3$ characterized by alternating layers of SrO and TiO_2**
  - Stoichiometric layers
- **Layers in (001) direction of anatase TiO_2 has the same structure as in $SrTiO_3$**
- **Nearly coherent interface**

Structure of as-grown $TiO_2/SrTiO_3$ interface

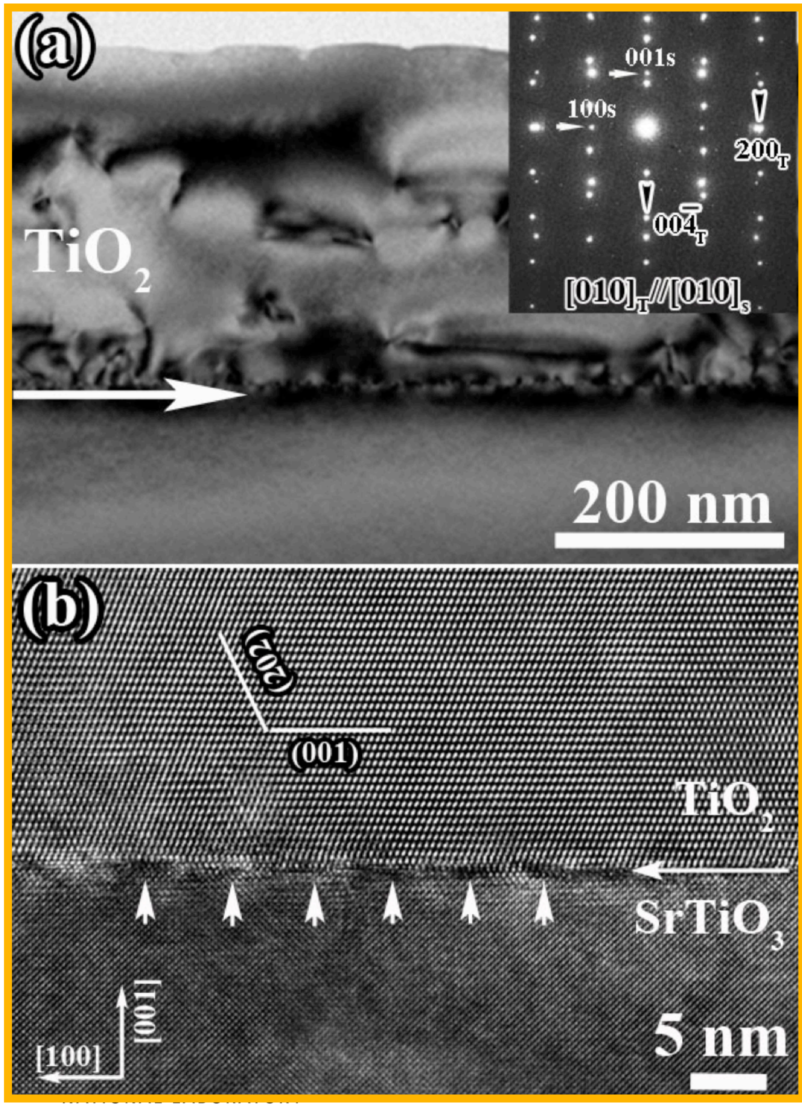

- **Epitaxial [004]-oriented TiO_2 film on (001) $SrTiO_3$**
  - Deposited via pulsed laser deposition
  - XRD confirms TiO_2 is anatase polymorph
  - Film about 300 nm thick
- **Sharp $TiO_2/SrTiO_3$ interface**
  - Misfit dislocation spacing: 5.6nm
- **Orientation relationship:**

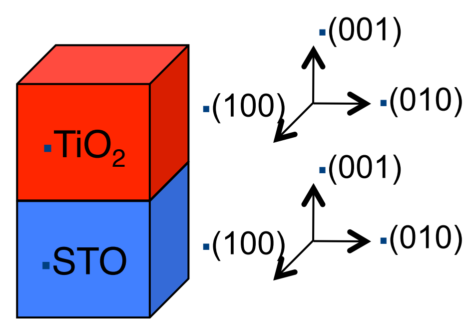

M. Zhuo, *et al.*, *Scripta Mat* **65**, 807 (2011).

Irradiation of $TiO_2/SrTiO_3$ interface

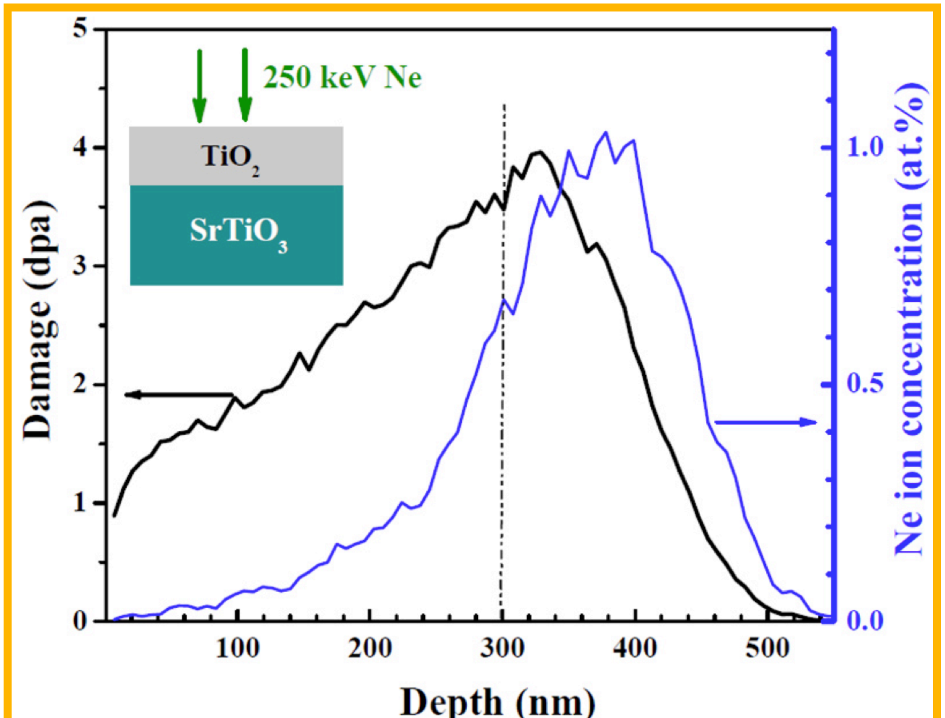

- **250 keV Ne irradiations**
- **Peak dpa is at about 330-340 nm**
  - About 30-40 nm deeper than interface
- **Films irradiated to $3.3x10^{15}$ to $1.7x10^{16}$ ions/cm^2**
  - Corresponds to 1-6 dpa at interface, based on SRIM

M. Zhuo, *et al., Scripta Mat* **65**, 807 (2011).

Irradiation of $TiO_2/SrTiO_3$ interface: room temperature

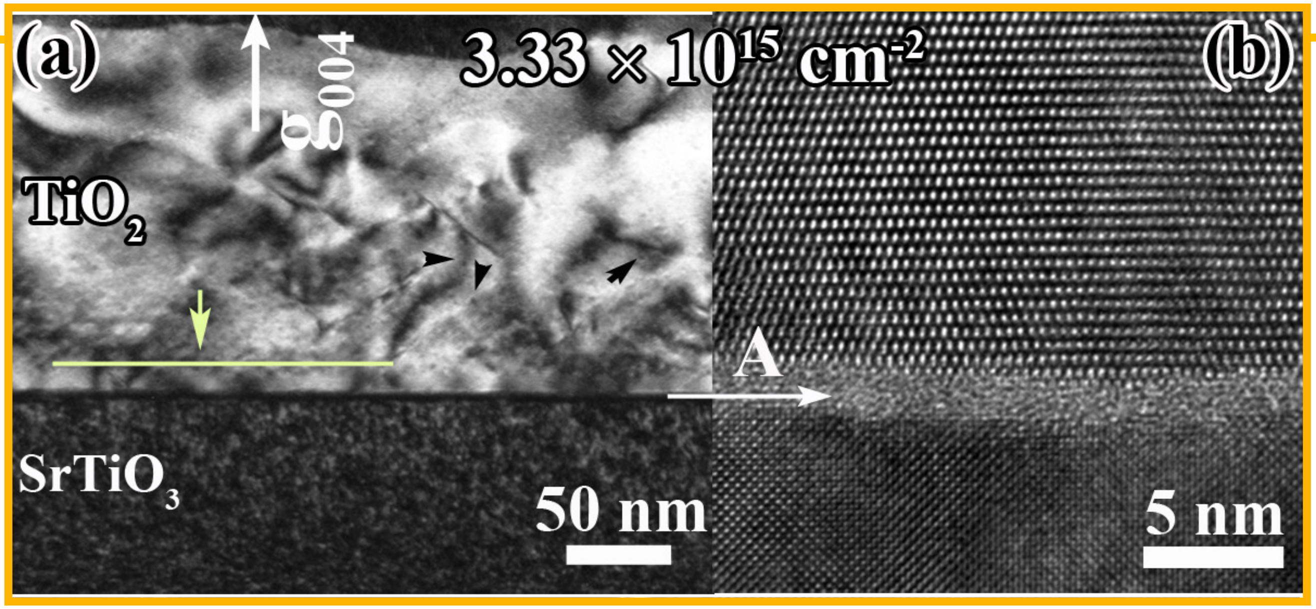

- **Denuded zone forms on TiO_2 side of interface**
- **Amorphous layer forms on $SrTiO_3$ side of interface**
- **Denuded zone persists even as amorphous layer forms**
- ***Denuded zone independent of atomic structure of interface***

M. Zhuo, *et al.*, *Scripta Mat* **65**, 807 (2011).

Irradiation of $TiO_2/SrTiO_3$ interface: 500 C

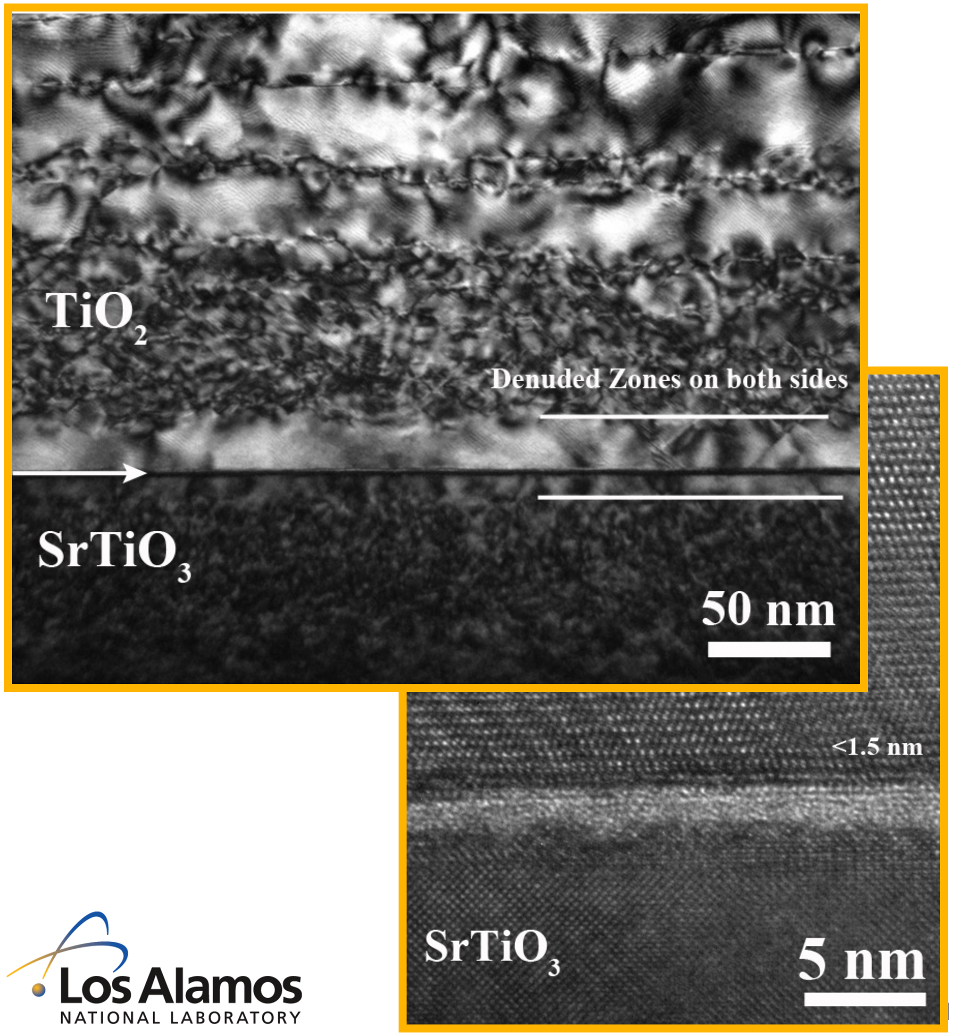

- **Denuded zone forms on *both* sides of the interface**
- **Very thin amorphous layer forms at the interface**
- **Dislocation walls form in TiO_2 thin film**

M. Zhuo, *et al., manuscript in preparation.*

Two determiners of defect properties near structureless interfaces

- **Defect transport driven by differences in chemical potential μ**
  - Defects move from regions of high chemical potential to regions of low chemical potential
- **Defect transport controlled by bulk migration energies**
  - Whether defects can cross interface depends on migration barriers relative to temperature in both phases

Two determiners of defect properties near structureless interfaces

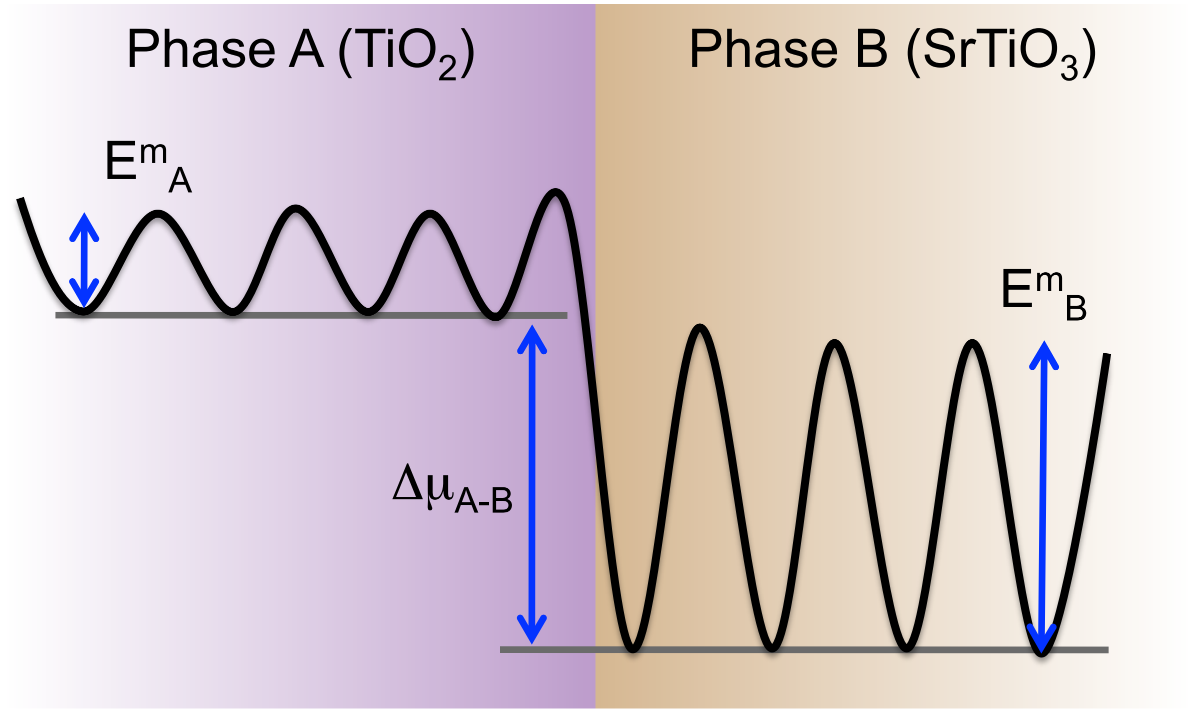

Towards a Figure of Merit for "structureless" interfaces

- **Differences in chemical potential μ drive defect flow from one side to the other**
  - Define phase A such that $\mu_A > \mu_B$
- **Differences in mobility E^m determine rate of defect buildup at interface**
- ***Kinetic sinks***

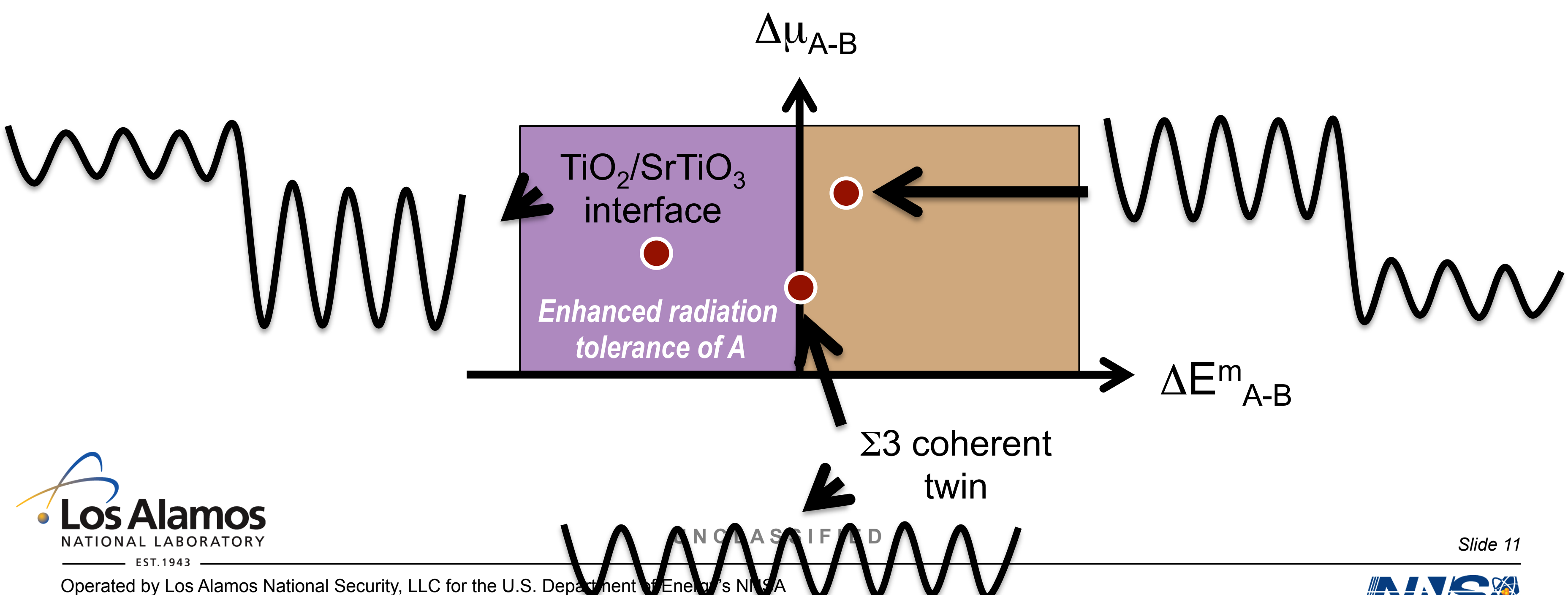

Kinetic Monte Carlo model for structuraless interfaces

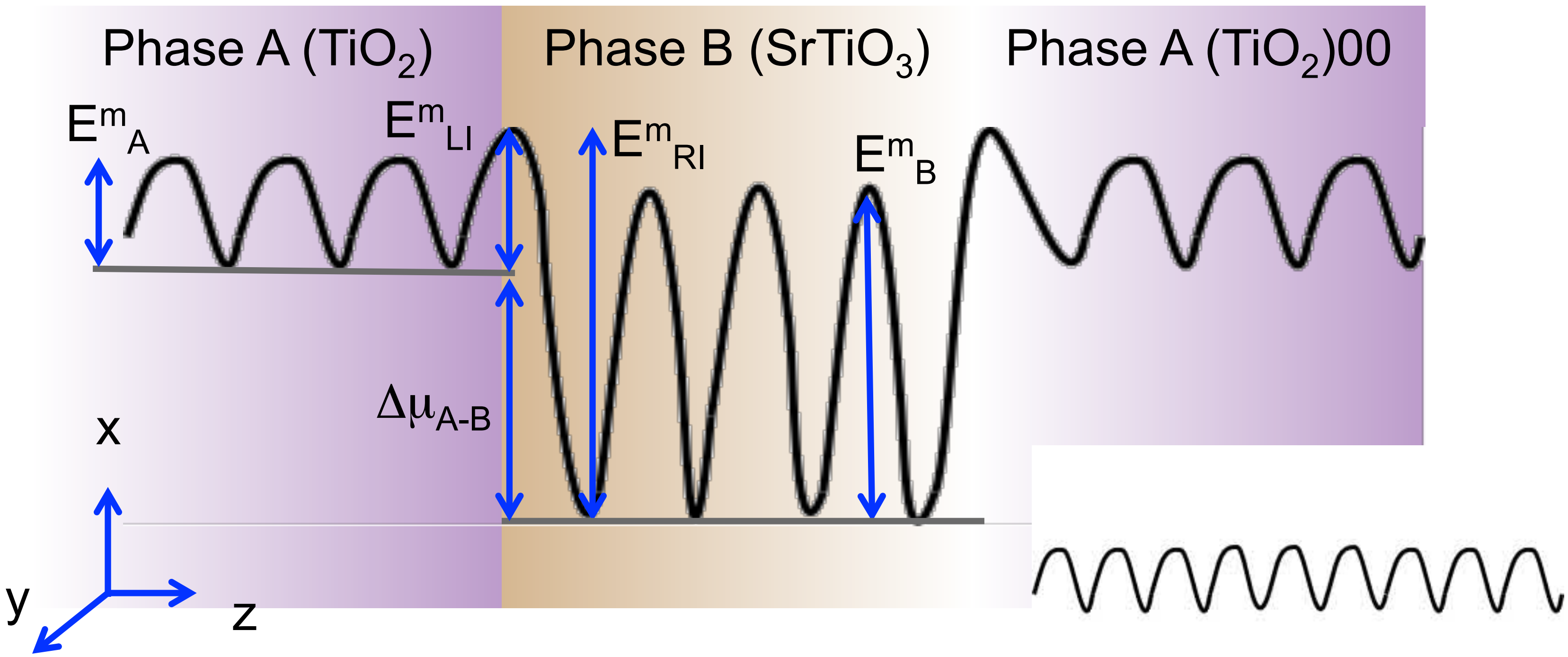

We have systematically change the migration parameters, run 1000 KMC independent calculations for each set and calculate the resulting defect profile.

Concentration profiles

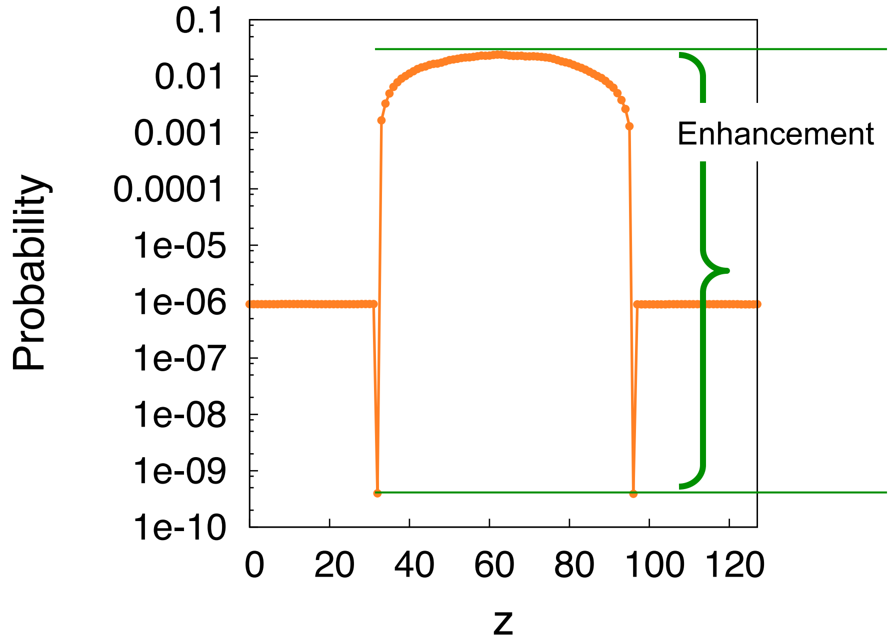

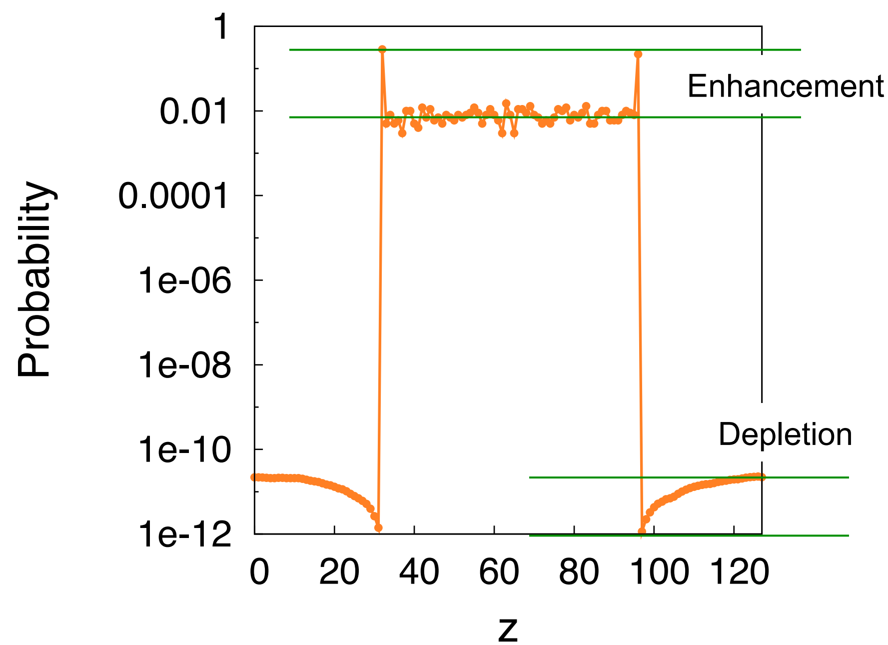

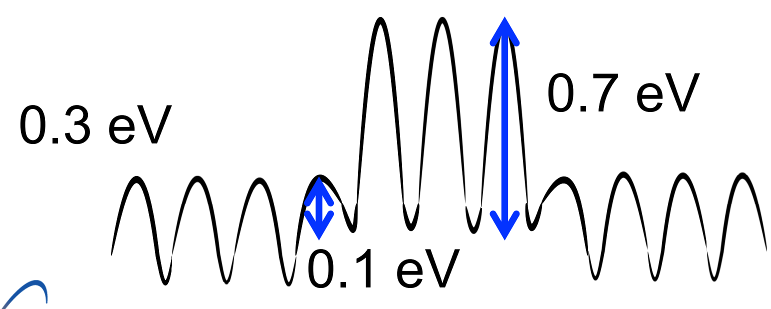

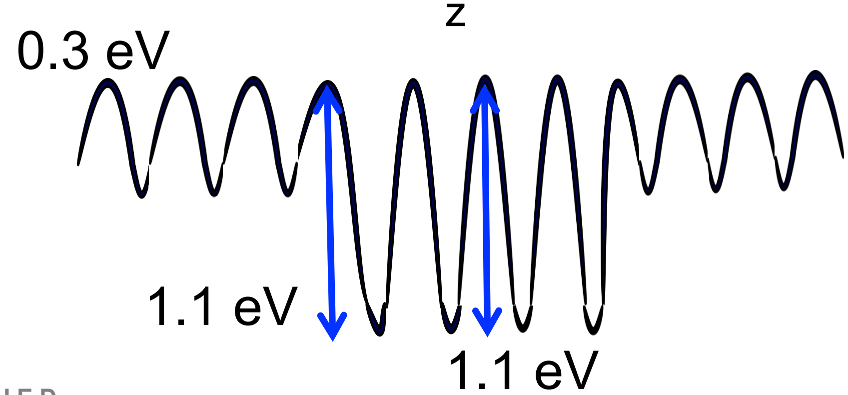

Δμ – ΔE maps at 300 K

The depletion probability is related to the length of the denuded zone

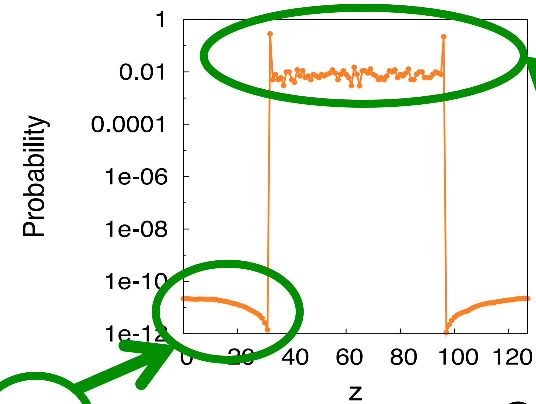

The enhancement probability is related to the amorphization

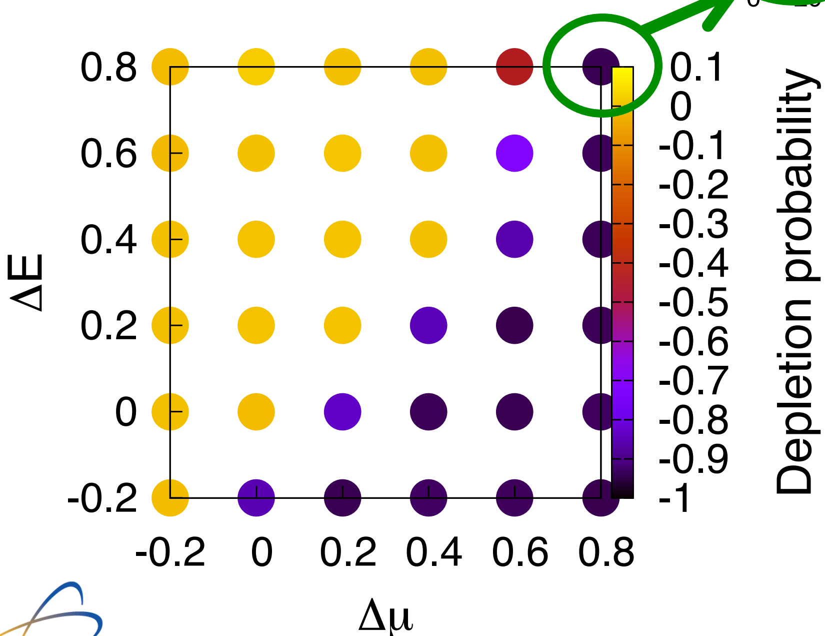

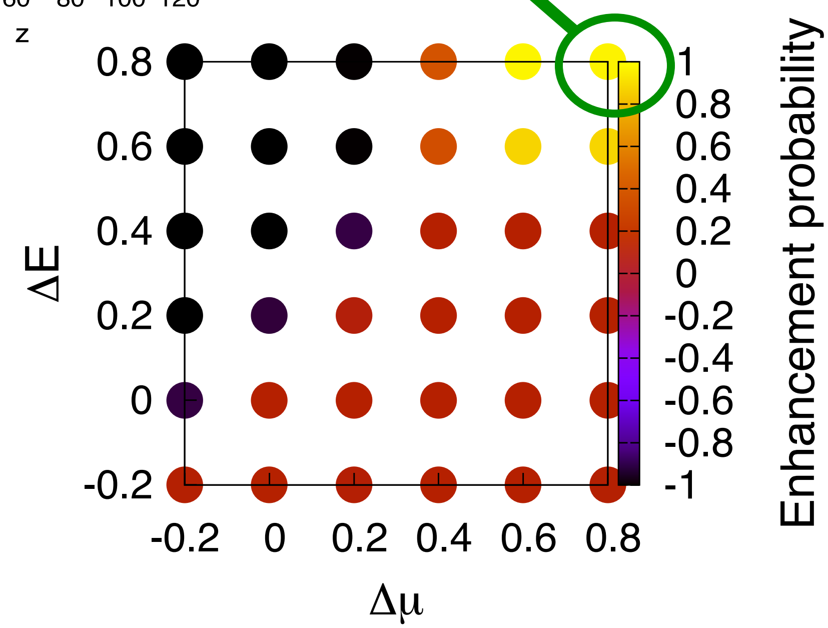

$\Delta\mu - \Delta E$ maps at 800 K

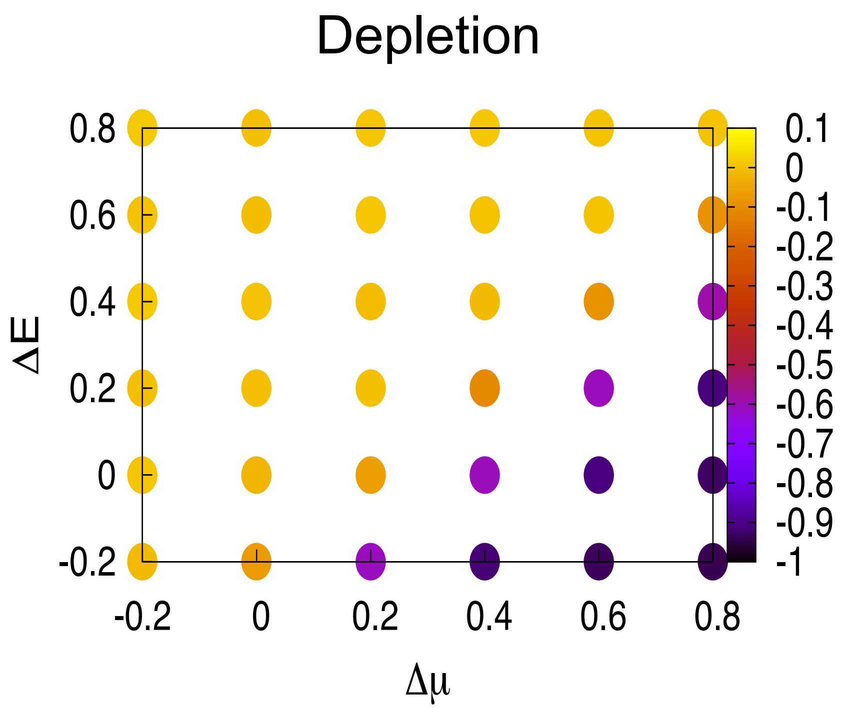

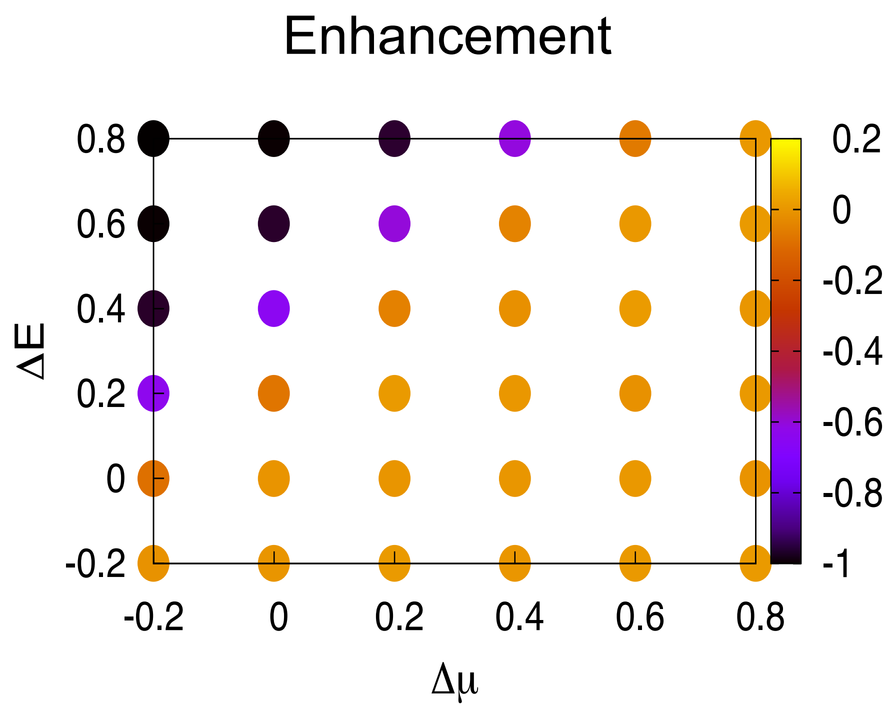

Increasing the temperature reduces the effect. It is a steady state effect

Two Reacting Defects at 300 K

Landscape Defect 1

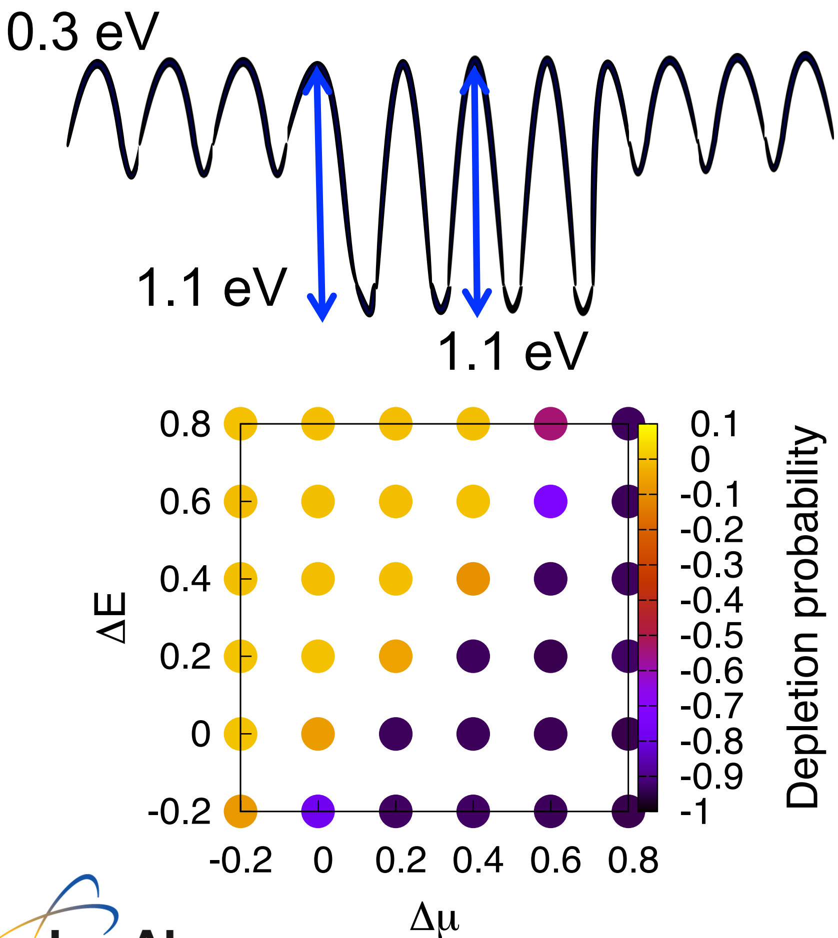

Landscape Defect 2

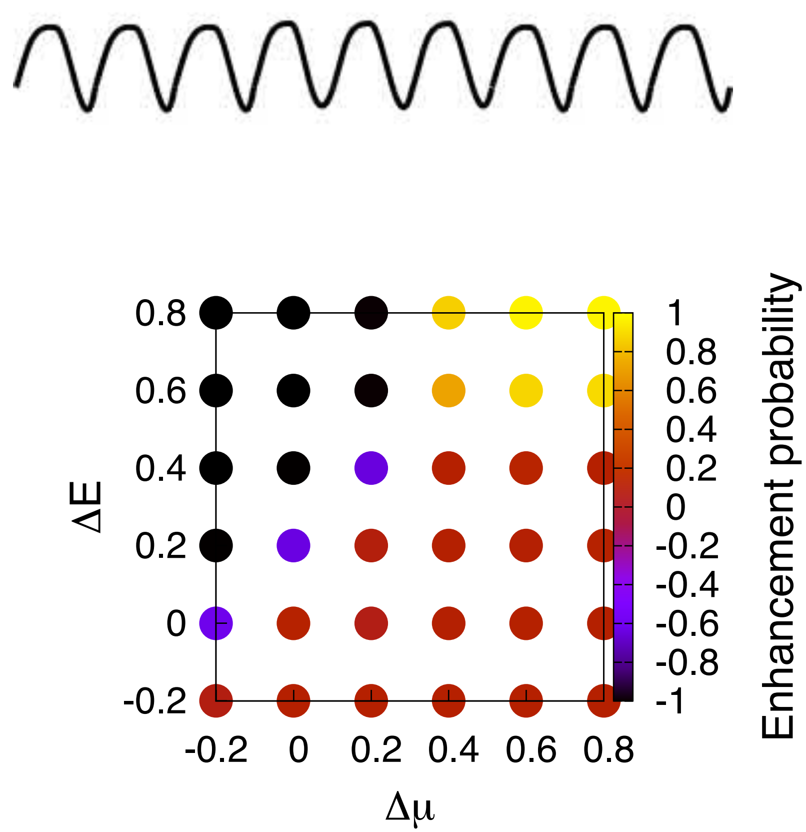

Reaction Probability at the Interface

Probability of reaction at the interface provided that a reaction has taken place

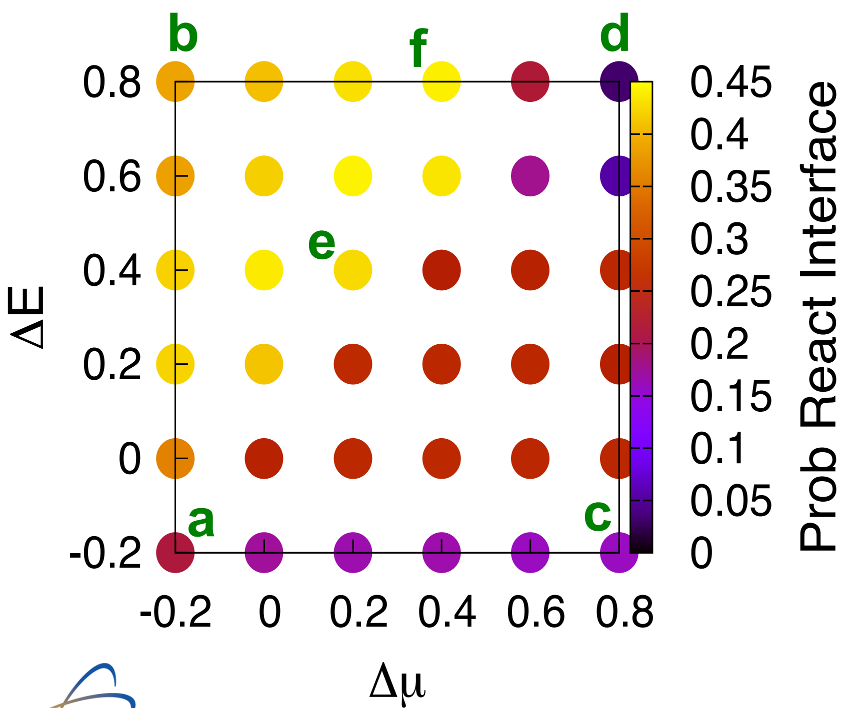

Total Probability of Reaction

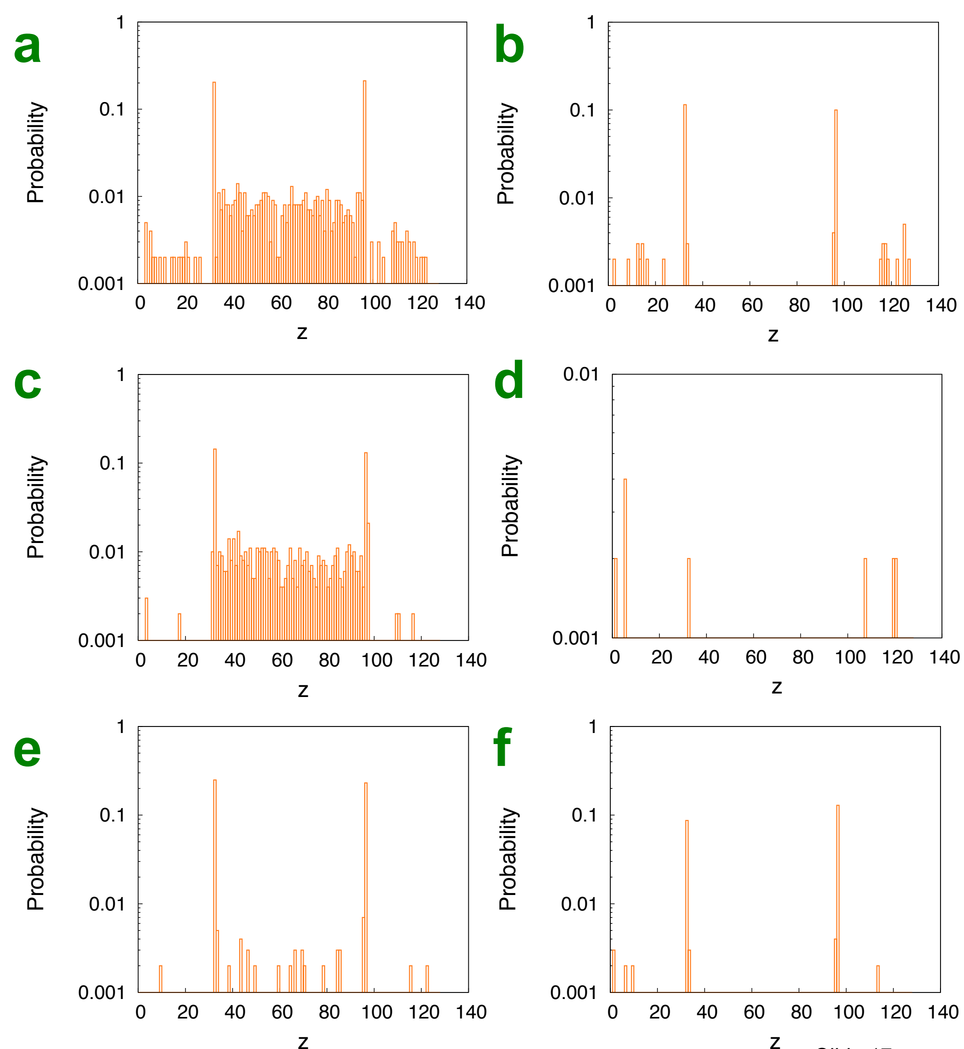

Two Reacting Defects at 300 K

Landscape Defect 1

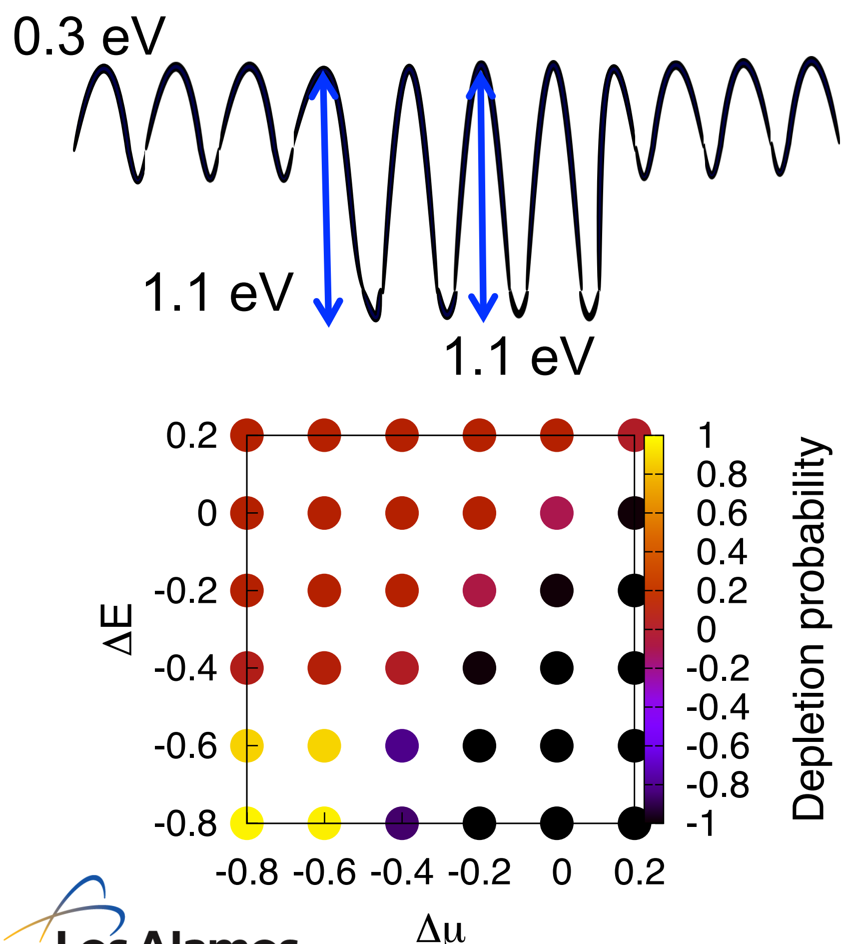

Landscape Defect 2

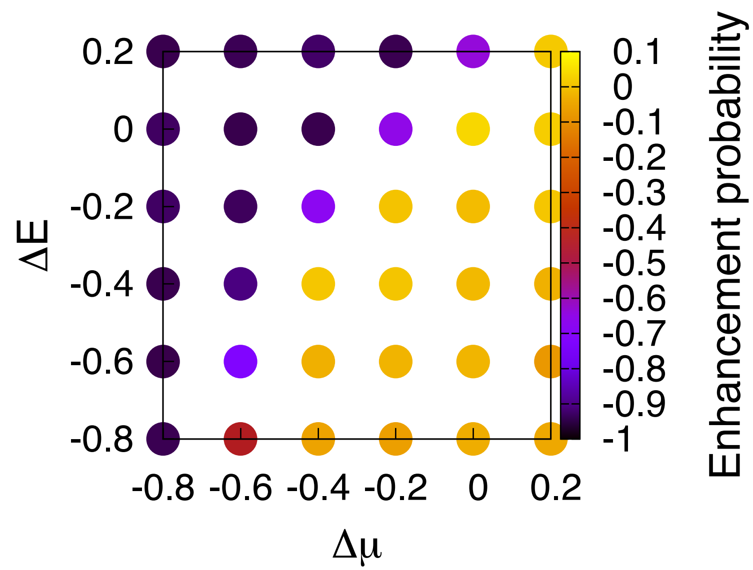

Reaction Probability at the Interface

Probability of reaction at the interface provided that a reaction has taken place

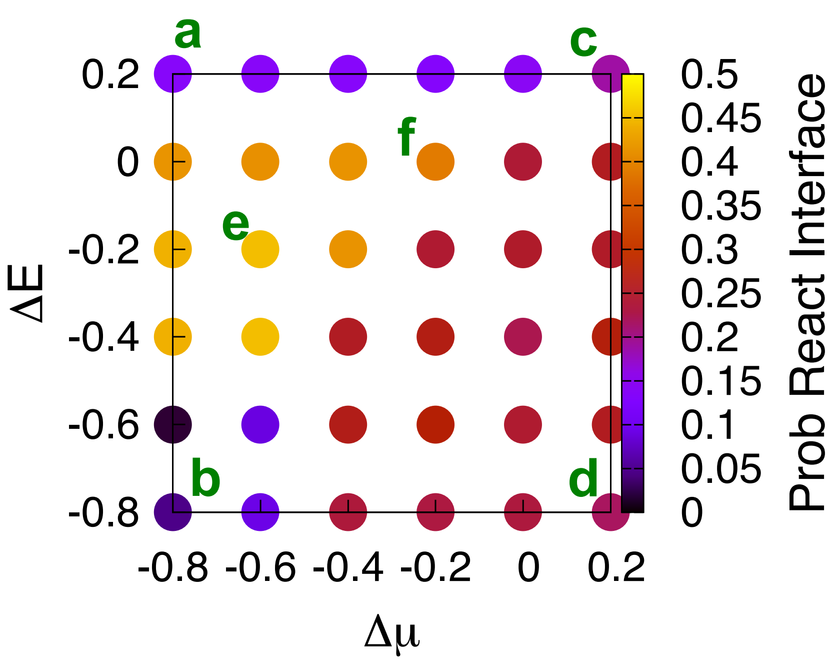

Total Probability of Reaction

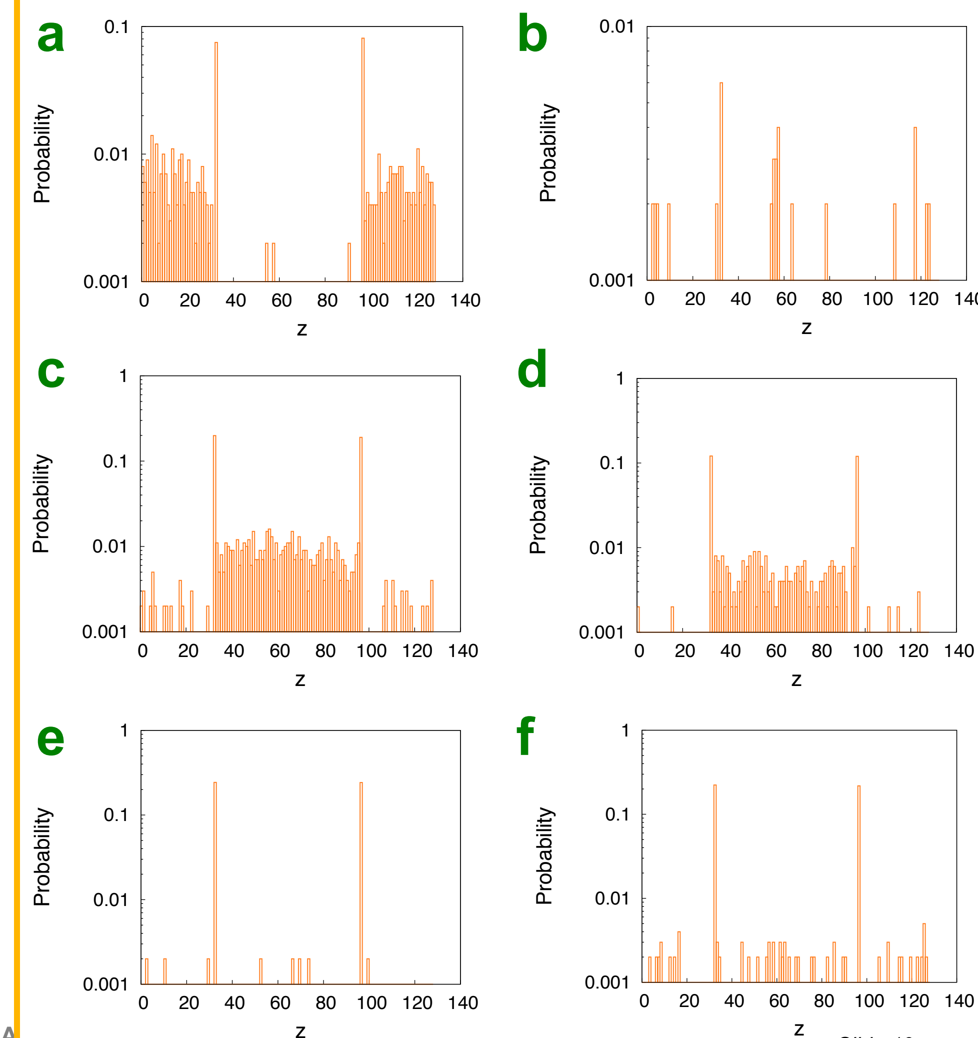

Motivation

Sink behavior of Interfaces

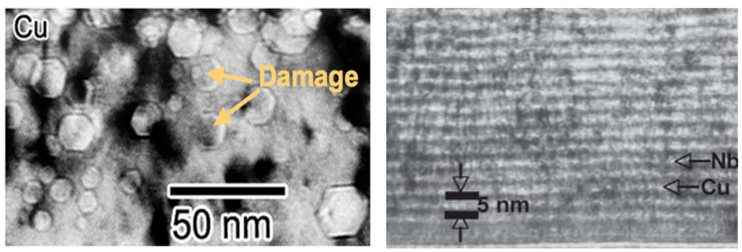

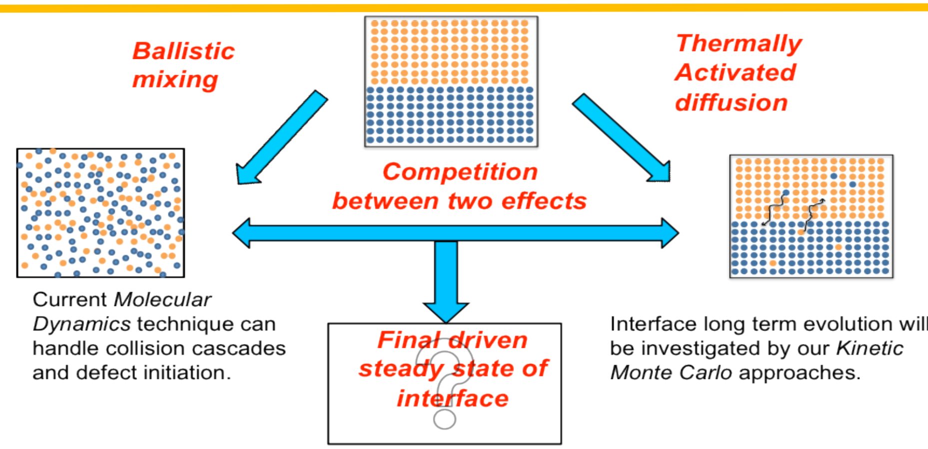

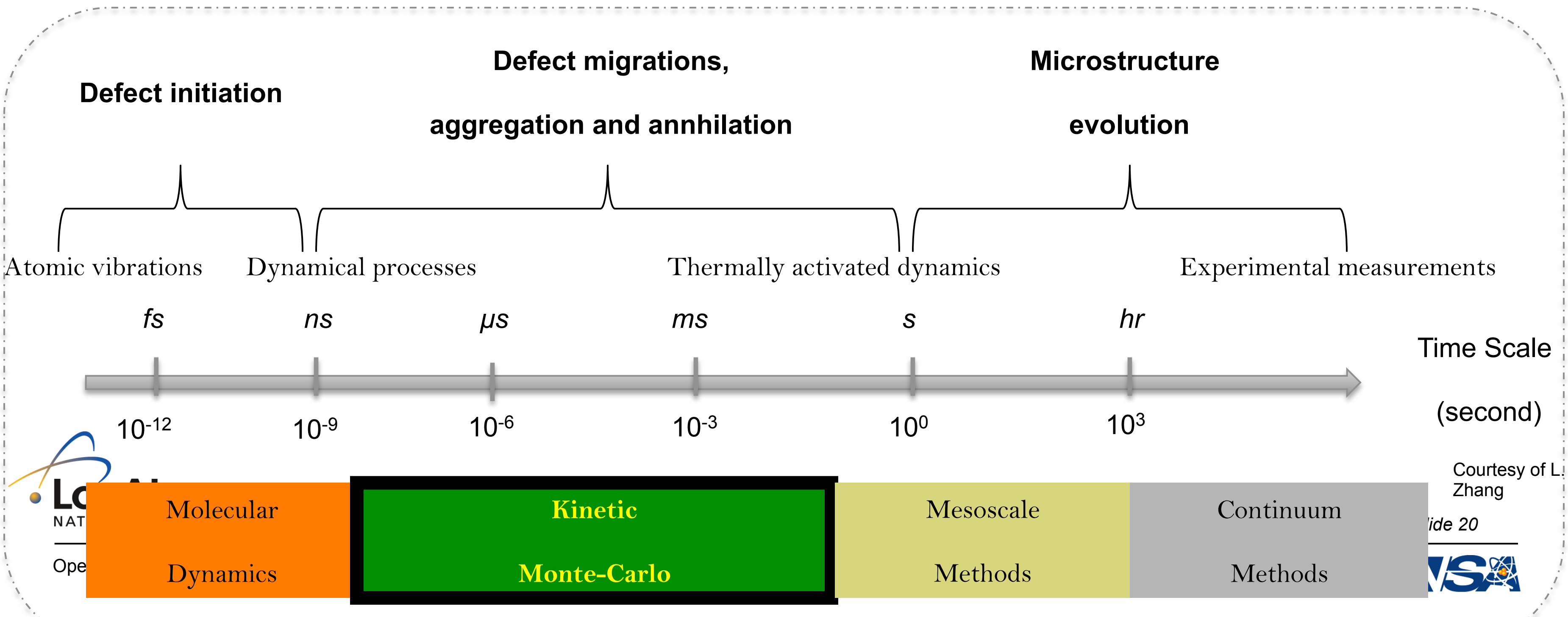

Courtesy of L. Zhang

Our Kinetic Monte Carlo Approaches

- **Self-learning KMC. (L. Vernon, B. Uberuaga, A. Voter)**
  - Dynamically explores the potential energy surface to discover all processes.
  - Calculate the rates accurately.
  - Might be computationally demanding.

- **Event-driven KMC. (Me and Alfredo)**
  - Uses the local microstructure to guess potential processes.
  - The accuracy in the rate calculation can be tuned.
  - Computationally less demanding.

Event-Driven KMC: Coupling MD LAMMPS – KMC

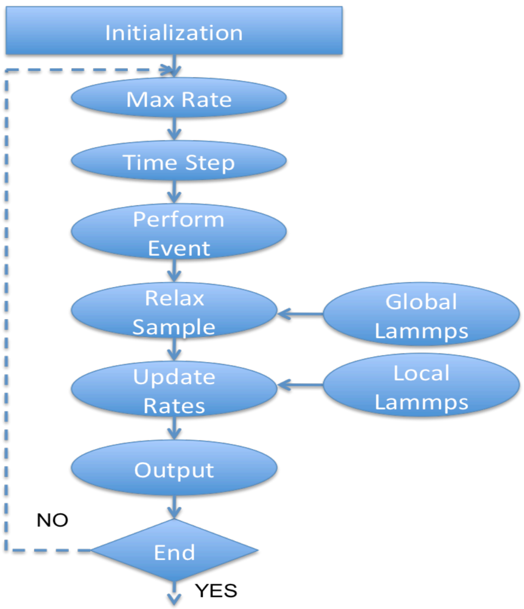

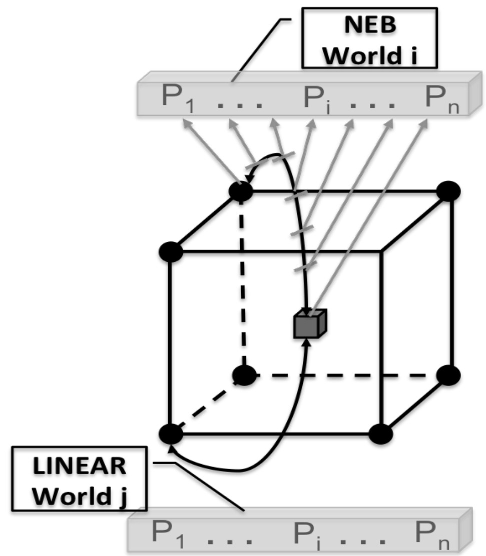

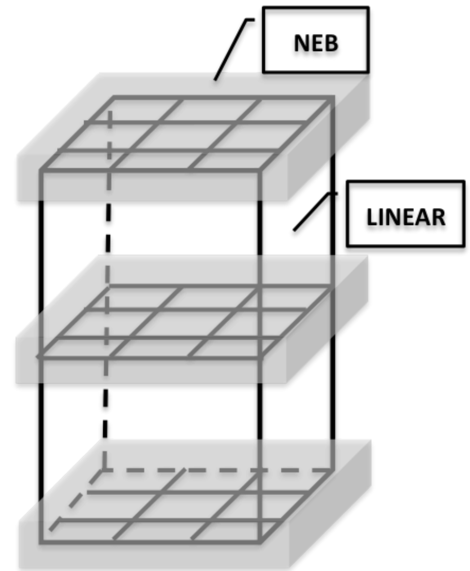

Set of possible events
Harmonic Transition State Theory
Particle rate: $\Gamma = \nu \exp(-E_{SP}/kT)$; Two options to calculate E_{SP}:

1. Linear approximation $E_{SP} = E_0 + (E_f - E_i)/2$
2. Nudged-elastic band (NEB)

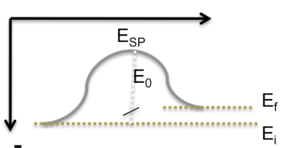

Each vacancy exchange is handled by a set of processors. The global relaxation is performed using all processors

Hybrid models can be used depending on the complexity of the sample to obtain more accurate results

Applications

- **(110) 4-degrees Twist Boundary in bcc Fe.**
  i. Interface structure
  ii. Vacancy formation energies
  iii. Vacancy accumulation using hybrid linear approx-NEB

- **(111) 2-degrees Twist Boundary in fcc Cu.**
  i. Interface structure
  ii. Vacancy formation energies
  iii. Vacancy accumulation using hybrid linear approx-NEB

Vacancy-Twist Boundary Interaction Energy in a (110) Fe Interface

Dislocation structure at the interface: 2 sets of $a_0/2<111>$ dislocations and 1 set of $a_0<100>$ screw dislocations

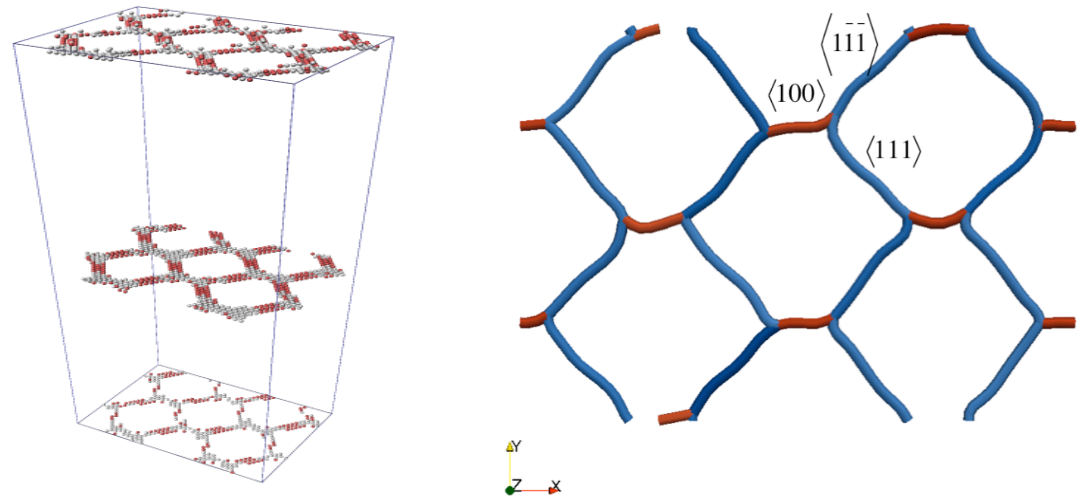

Interaction energy maps. Vacancies are attracted to dislocations. Thermodynamic driving force for the vacancies to accumulate at the interface.

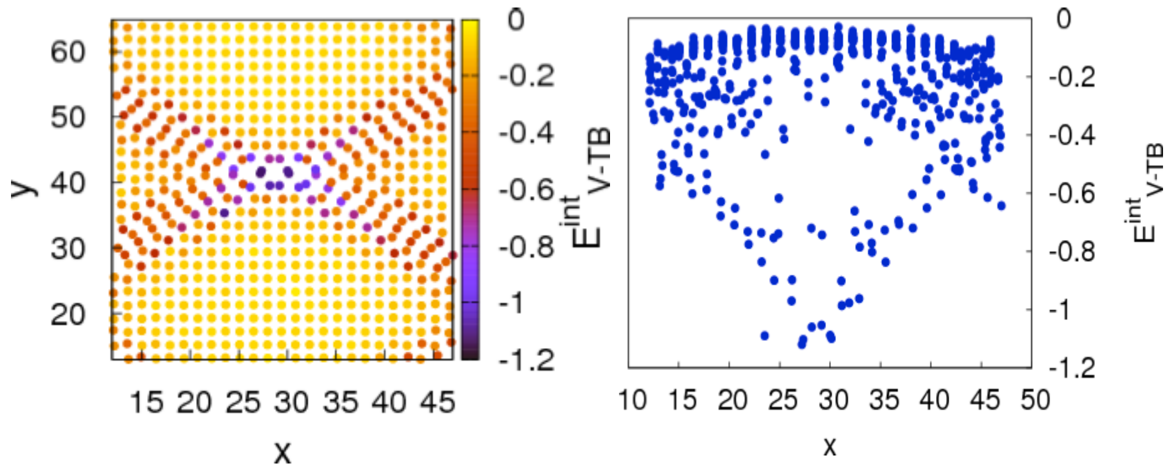

The interaction energy is most attractive at <100> segments forming the MDIs

Vacancy accumulation at the (110) Fe Interface

- vacancies
- Non-bcc atoms

$\Phi=10^{-4}$ V/A^3.s=1.16 10^{-3} dpa

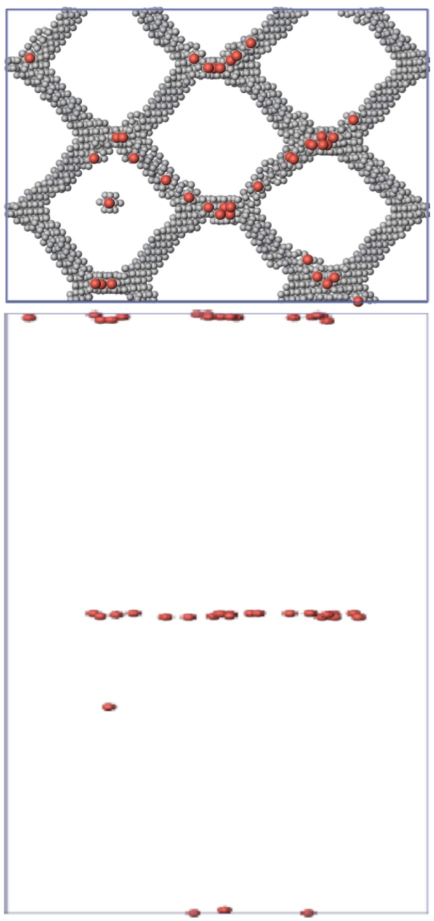

$\Phi=10^{-3}$ V/A^3.s=1.16 10^{-2} dpa

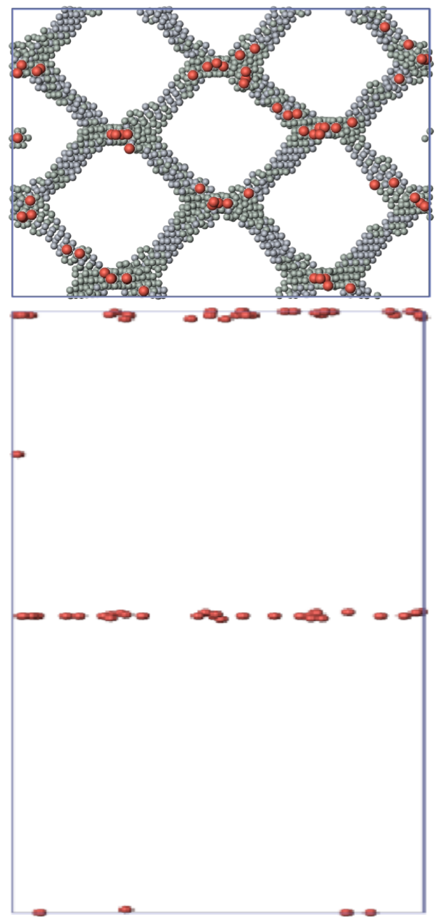

$\Phi=10^{-2}$ V/A^3.s=1.16 10^{-1} dpa

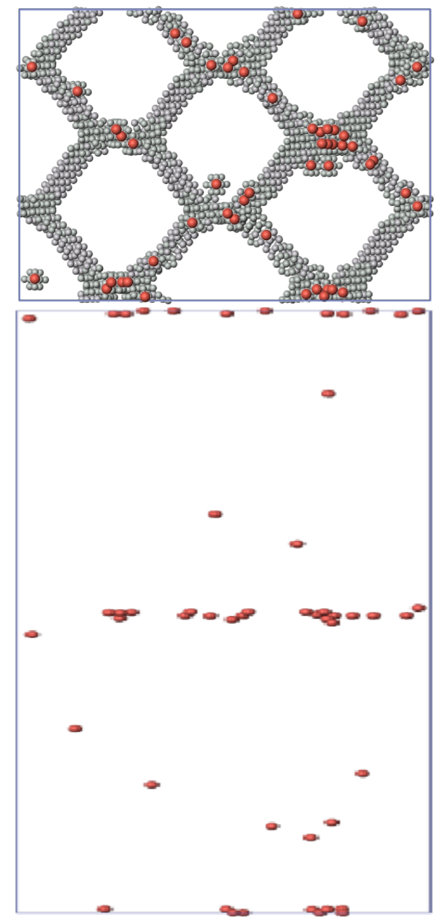

Vacancies decorate the more energetic <100> segments forming the MDIs

Error Estimation

MD annealing for 1 ns at 500 K of KMC samples computing atomic displacements and maximum shear strength

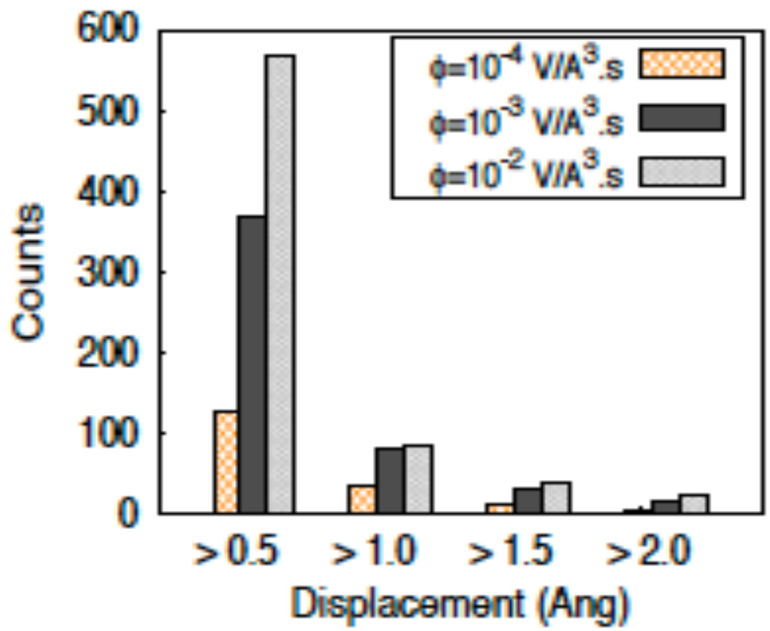

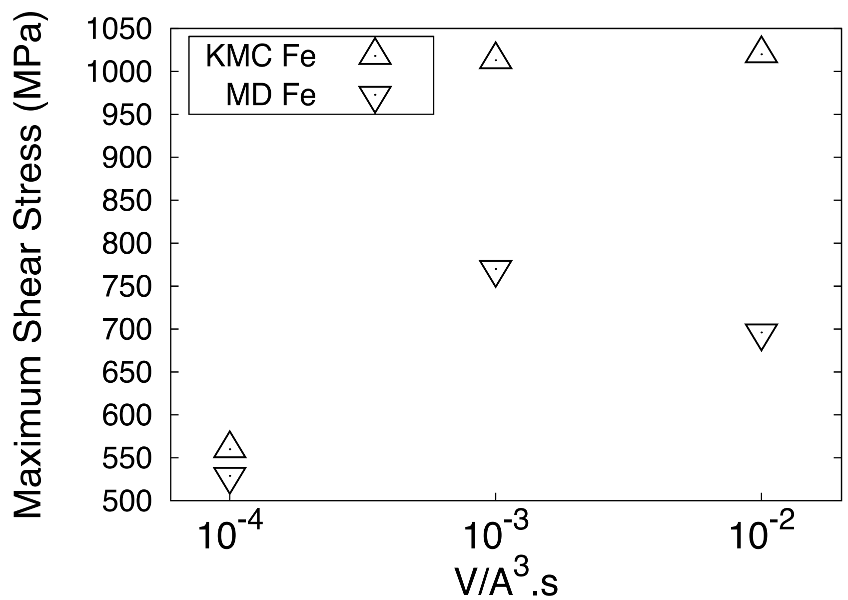

For the lowest dose rate investigated the number of events does not change the observable of interest. On the other hand, for larger dose rates, the maximum shear stress is ~ 30% lower after annealing.

Vacancy-Twist Boundary Interaction Energy in a (111) Cu Interface

Dislocation structure at the interface: 3 sets of $a_0/6<112>$ Shockley partial screw dislocations

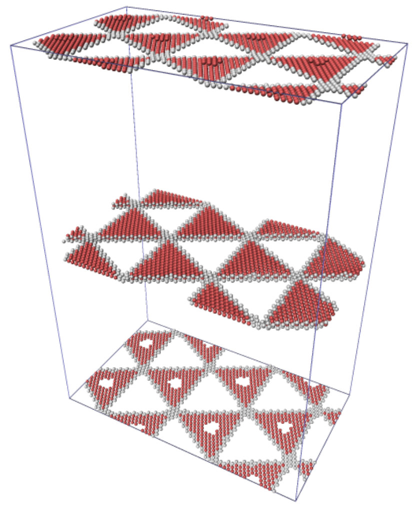

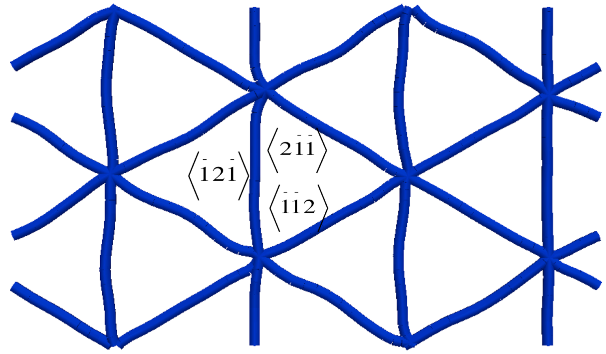

Interaction energy maps. Vacancies are attracted to dislocations. Thermodynamic driving force for the vacancies to accumulate at the interface.

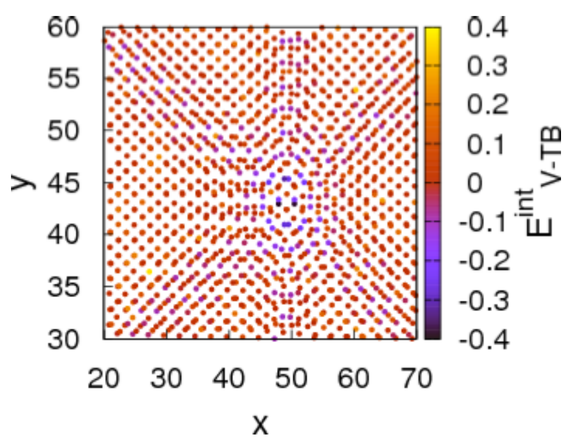

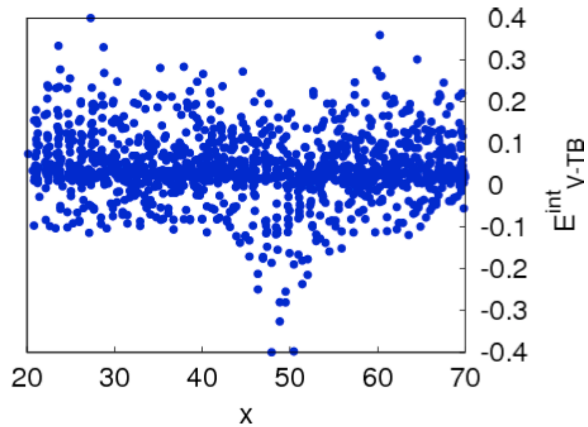

The interaction energy is most attractive at the MDIs

Vacancy accumulation at the (111) Cu Interface

- vacancies
- Non-fcc atoms

$\Phi=10^{-4}$ V/A^3.s=1.17 10^{-3} dpa

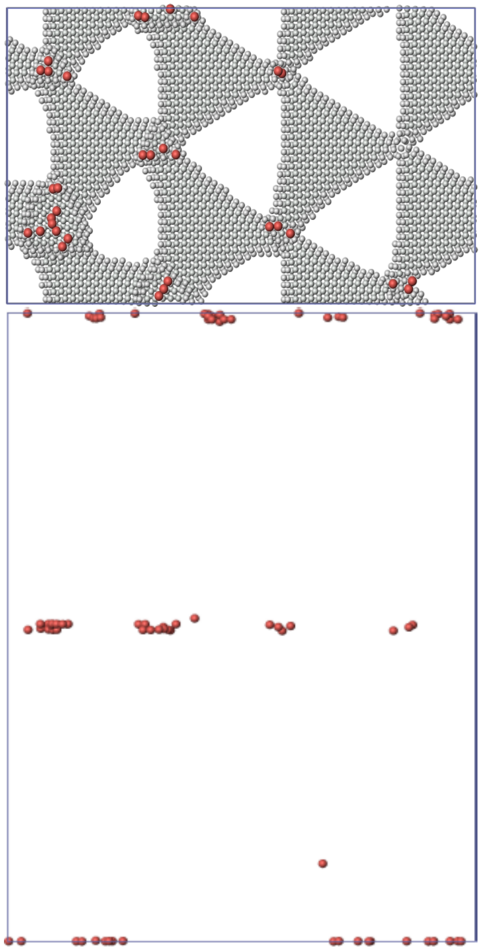

$\Phi=10^{-3}$ V/A^3.s=1.17 10^{-2} dpa

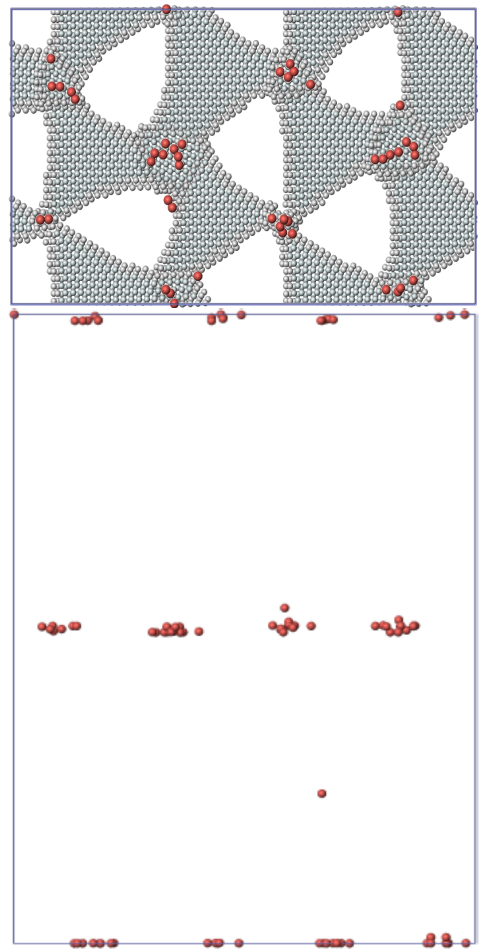

$\Phi=10^{-2}$ V/A^3.s=1.17 10^{-1} dpa

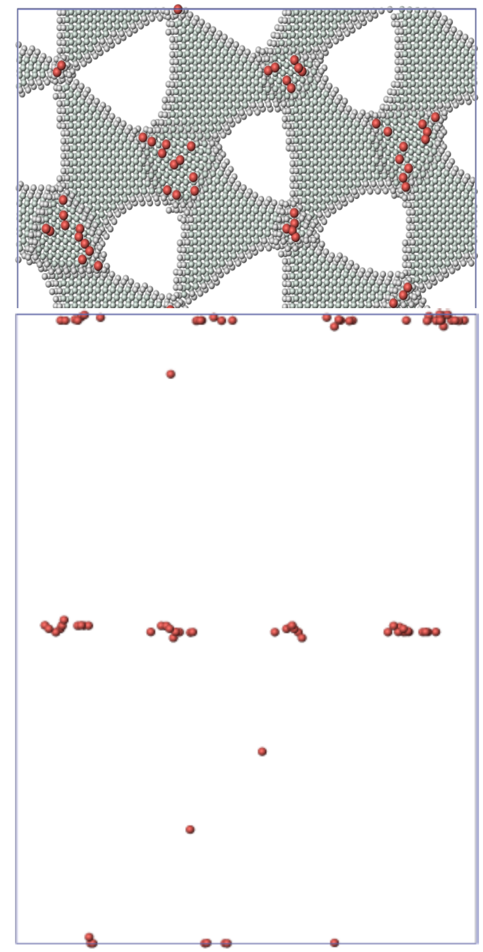

Vacancies agglomerate at the MDIs changing the dislocation structure

Error Estimation

MD annealing for 1 ns at 500 K of KMC samples computing atomic displacements and maximum shear strength

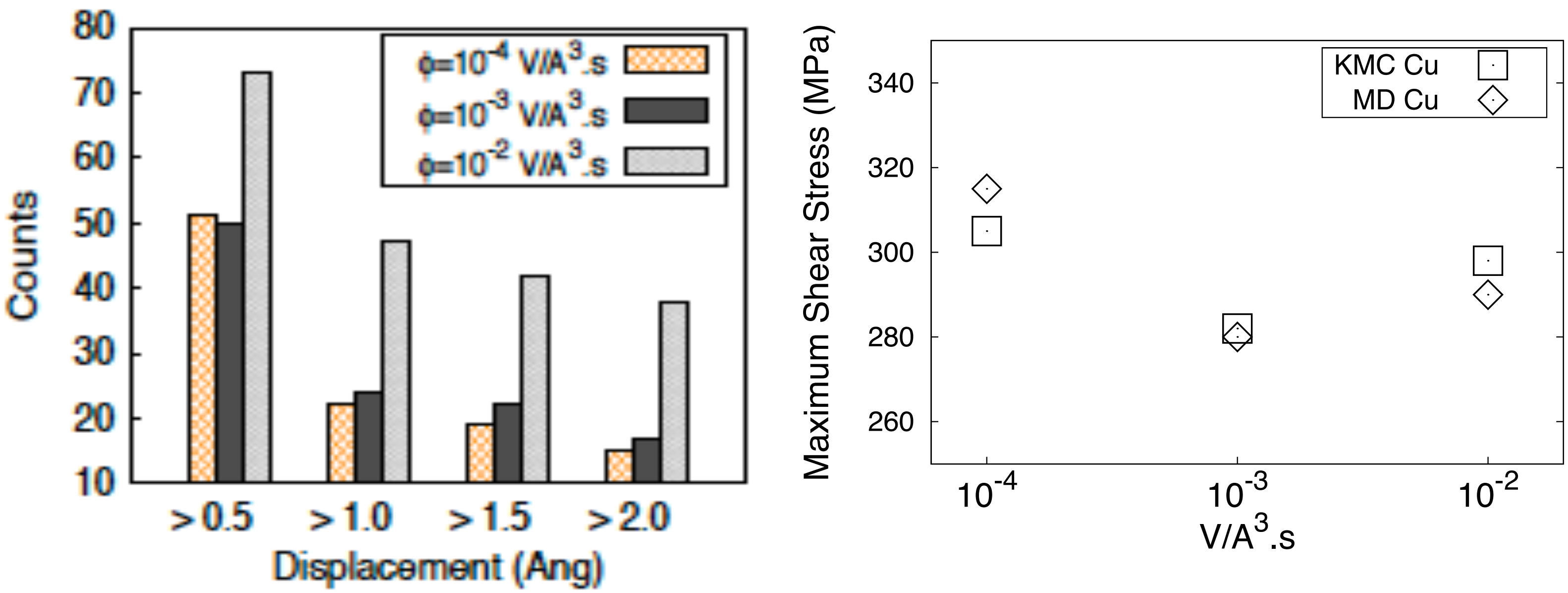

In this case the events do not change the observable of interest at any dose rate. The maximum different in the shear stress is ~ 3%.

Conclusions

- We have developed an hybrid KMC-MD off-lattice algorithm
- It is able to describe diffusion with all the fields (elastic, thermodynamic)
- We can reach real times far beyond MD capabilities.
- Application to CuNb interfaces (in collaboration with Liang Zhang-MIT).
- Improvement of the physics:
    - Implementation of interstitial diffusion.

Acknowledgements: Work supported at LANL by the DOE's Energy Frontier Research Center for Materials under Irradiation and Mechanical Extremes (CMIME), and by the LDRD program